

Design and Analysis of Indium Gallium Nitride Based PIN Solar Cell

Maithili Kumbhare*, P. Sathya**†

*Department of MEMS and Sensors, School of Electronics Engineering, VIT University, Vellore, Tamil Nadu, India

**Assistant Professor, Department of MEMS and Sensors, School of Electronics Engineering, VIT University, Vellore, Tamil Nadu, India

(maithu.kum@gmail.com, p.sathya@vit.ac.in)

†P. Sathya, Tel: 9790902453,

Received: 16.05.2016 Accepted:16.08.2016

Abstract- The main objective of this paper is to design and simulate a high efficiency quad junction PIN solar structure using group III-nitride material system. Out of the nitride family, Indium Gallium Nitride alloy possesses a direct and wide energy band gap ranging from 0.7 eV for Indium Nitride up to 3.4 eV for Gallium Nitride, because of which it covers most of the solar spectrum thus serving as a wide band gap top cell in a mechanically stacked or a bounded multi-junction hybrid solar cell. Hence this material is chosen here to design wide band gap Quad junction device. The PIN structure is built as a quad layer solar cell cascaded using tunnel junctions. For $\text{In}_x\text{Ga}_{1-x}\text{N}$, the mole fraction values of Indium (x) are altered for the individual cell layer. The mole fraction variation leads to the change in the grading of the concentration of Indium along the depth of the structure. Variable bandgap is achieved by varying the grading, thus making the multijunction cell to be a wide energy bandgap structure. For each cell, the parameters are modelled numerically and simulated for mole fraction values (x) of 0.365, 0.525, 0.70 and 0.93. The individual cell analysis is performed and then the structure is cascaded together to form a 100 cm^2 area quad junction solar cell for which the performance analysis is obtained as voltage to be 1.17 V/cm^2 and current to be 3.18 mA/cm^2 which accounts to a maximum conversion efficiency of 33.63% for 100 Watt/cm^2 , 1.5AM one sun spectrum illumination.

Keywords Quad junction, PIN structure, GaN, InGaN, grading, thickness optimization, PC1D.

1. Introduction

The limited energy resources and its harvesting is the leading and growing industrial sector today. Solar energy, being available in abundance can cater the vast energy needs. To meet these enormous energy needs, maximum optimisation of materials is required. Multijunction solar cell serves this purpose better. Multijunction solar cells from tandem solar cells [1] to quad junction solar cells with quantum dots are being fabricated and implemented in real time for desired applications [2]. A rare earth group V material Erbium Arsenide (ErAs) is used as a tunnelling material; helping junctions to withstand thermal energy stability[3]. PIN structure is proposed to deal with most two critical issues; i.e. degree of polarization and improving conversion efficiency. Numerically simulated structure show characteristics with high efficiency and less effect to degree of polarization [4]. Piezoelectric polarization affect the crystal quality; energy band gets tilted towards the detrimental direction for carrier collection. With increase in

the value of mole fraction of Indium, this effect grows more serious along the growth of the crystal structure [5]. Hetero interfaces and polarization affect the crystal performance if Indium composition is high. So, step graded interlayers are developed and their thickness and p type doping concentration are investigated [6]. Introducing intrinsic layer between amorphous silicon and crystalline silicon substrate enhances efficiency, creating back surface field (BSF) leading to increase in conversion efficiency by 2%; giving around 21.05% efficiency for optimised yet small thickness value [7]. Multiple Quantum Well (MQW) solar cell are more efficient than p-i(bulk)-n solar cells. Taking polarization effects into account, the temperature dependence of open circuit voltage and short circuit current are investigated, giving 35% conversion efficiency. Additionally, increase in temperature leads to increase in open circuit voltage and short circuit current [8]. InGaN/GaN PIN structure with 10.8% grading value with ITO spreading layer gives quantum efficiency of 74.1% but conversion efficiency less than 10% [9]. PIN solar cell is simulated with

Indium fraction (x) varying from $x = 0.07$ to 0.25 ; numerical modelling of the cell is done by employing PC1D thus proving $x = 0.2$ fraction value to give better conversion efficiency in the range. [10] Solar cell heterojunction structure p-GaN/ n- $\text{In}_x\text{Ga}_{1-x}\text{N}$ is simulated using a finite element approach. Tandem cell structure is p-GaN/n- $\text{In}_{0.5}\text{Ga}_{0.5}\text{N}$ /p-Si/n-Si; predicting 28.98% efficiency with thickness and doping concentration of graded region affecting performance of the cells [11]. Using APSYS (Advanced Physical Models of Semiconductor Devices), variable Indium gradient layer interface is created between Indium nitride and Gallium nitride. Modelling and integrating absorption coefficient of Indium nitride, fabrication is done by metal organic chemical vapour deposition (MOCVD) method. Results state that effective variation of mole fraction of Indium and proper thickness optimization for hybrid InN/InGaN structure enhances performance of current nitride based solar cells [12]. Theoretical study proves the efficiency of heterojunction devices is up to 11%; also homojunction devices with highly doped p type InGaN layers with proper thickness are grown. Because of improved cell concentration, p type nitride cells can be grown with high efficient InGaN solar cell [13]. N type rich concentration MBE (Molecular Beam Epitaxy) growth at low temperature facilitates growth of InGaN films, which are 10% and 20% thick. But, this leads to the problem of current leakage with larger cell area of devices. The tandem heterojunction cell gives 22% efficiency for larger area analysis [14]. Comparative study of InGaN/GaN heterojunction and InGaN homojunction solar cell is done based on parameters such as open circuit voltage, short circuit current, fill factor and conversion efficiency based on variation in mole fraction value of Indium concentration, thickness, background doping of InGaN layer. The efficiency achieved is 11.3% for a single PIN InGaN/GaN heterojunction solar cell with 0.45 as the Indium concentration fraction, whereas the single homojunction solar cell gives approximately 17% efficiency for the same parameters [15]. PIN InGaN discontinuous nano rods with metal layers and their photovoltaic characteristics are studied. Results show low conversion efficiency but high short circuit density of $4.6\text{mA}/\text{cm}^2$ under standard one sun, 1.5AM spectrum illumination. This high current is because of improved crystal quality and better light concentrating effects [16]. Analytical approximation of d_{\min} is done; stating that open circuit voltage, short circuit current and fill factor saturate at a level when d_{\min} (thickness of InGaN layer) is exceeded. i-GaN layer is added between p and i- InGaN to obtain quality hetero interface. 2D electron gas formation at the n-GaN/i-InGaN interface improves quantum efficiency [17]. Parametric analysis of lattice structure of GaN/InGaN PIN solar cell on GaN substrate is done. Parameters are simulated as a function of GaN/InGaN quantum well number. Multiple quantum well with 28 wells, $1.193\text{mA}/\text{cm}^2$ of current density give 1.05% conversion efficiency. Backdrop is wider absorption of spectrum is not achieved. Hence, InN quantum dots in photovoltaic device may help with better and wider absorption [18]. TCAD (Technology Computer Aided Design software) is used to simulate the structure with compositional grading from 0 to 0.11; thus increase in short circuit current density, open circuit voltage

because of high carrier collection due to low band offset at the junction and high band bending in the intrinsic layer. Results obtained are $2.21\text{V}/\text{cm}^2$, $0.99\text{mA}/\text{cm}^2$ with 77% fill factor under standard solar conditions [19]. InGaN/AlGaN lattice solar cell is investigated with mole fraction value of Indium to be 20% and 40% for InGaN quantum wells. Results show 18.2% increase in short circuit current density obtained in $\text{In}_{0.4}\text{Ga}_{0.6}\text{N}$ with $\text{Al}_{0.2}\text{Ga}_{0.8}\text{N}$ because of increase in the electric field in absorption region. Improved carrier transport, thus increase in carrier collection efficiency, and thus better conversion efficiency [20]. Single heterojunction and double heterojunction samples of InGaN are grown using metal organic chemical vapour deposition (MOCVD), with variable thickness and recombination rate. Strain variation is different for single and double heterojunction. Higher strained double heterojunction shows droplets of Indium. No uniform replacement takes place between indium and Gallium atoms; thus quality of epitaxial layer is degraded [21]. A mathematical model for Ga-face GaN/InGaN hetero structure solar cell explaining piezoelectric polarization charges at interface improves efficiency of single hetero structure as compared to non-polar solar cell by 45%. This structure also has a solar unit for developing high efficiency multiple quantum wells (MQW) [22]. $\text{In}_{0.04}\text{Ga}_{0.96}\text{N}/\text{SiC}$ is designed and its performance is investigated using simulator ISE TCD. Performance evaluation involves parameters like open circuit voltage, short circuit current density, fill factor and efficiency. Conclusion states $\text{In}_{0.04}\text{Ga}_{0.96}\text{N}/\text{SiC}$ alloy is practically suitable for tandem cell applications [23]. Three types of InGaN based solar cells are simulated using AMPS (Analysis of Microelectronic and Photonic Structures) simulator i.e. simple junction, dual junction and triple junction. Numerical simulations lead to conclusion that out of 1.2 eV to 1.5 eV bandgap; optimization is done at 1.34 eV with 25.02% conversion efficiency. Efficiencies obtained for single junction are 25.02%, dual junction is 35.45% and triple junction is 42.34%. Analysis of GaN as tunnel junction material is done and is concluded that it has high thermal stability with temperature coefficient (TC) to be $-0.04\%/^{\circ}\text{C}$ [24]. Multiple quantum well InGaN based solar cells are fabricated using various electrode structures with nano dots of variable length and transparent coatings over it. Simulation show that solar cell with 50nm dot length provides up to 41% conversion efficiency under standard solar conditions, owing to the top reflecting transparent coating over the dot structure [25]. PIN InGaN/GaN structure is fabricated over a Ti/Ag mirror coated Si substrate enhancing the absorption from a multi reflecting surface with a thin absorption layer, providing 57% increase in the current density and improving the conversion efficiency from 0.55% to 0.80% [26]. Comparative study of two different grading values of mole fraction of Indium for $\text{In}_x\text{Ga}_{1-x}\text{N}$ multiple quantum well solar cells are studied, i.e. $\text{In}_{0.2}\text{Ga}_{0.8}\text{N}$ and $\text{In}_{0.28}\text{Ga}_{0.72}\text{N}$. $\text{In}_{0.28}\text{Ga}_{0.72}\text{N}$ face some structural defects leading to lower value of open circuit voltage than $\text{In}_{0.2}\text{Ga}_{0.8}\text{N}$ with fill factor value of 0.7. Results show that efficiency increases with temperature up to 100°C , later to which open circuit voltage decreases and short circuit current increases [27]. A quad junction solar cell using InGaN/GaN is theoretically proposed with variable mole fraction of

Indium value, providing the cell with the desired wide bandgap. With the thickness optimisation done, conversion efficiency of about 45% is achieved for 100 sun concentrated lens structure under 1.5 AM illumination spectrum. Issues such as detrimental effects, polarization, current mismatch, crystal quality are discussed and analysed [28]. Owing to all the literature work done, multijunction PIN structure will serve most of the issues and prove a better solution to all the real time problems faced in solar cell performance characteristics. So, a nitride material based quad PIN solar structure is proposed here to achieve high efficiency and absorption of complete solar spectrum.

2. Design Methodology

The quad junction device is designed and simulated in PC1D (Personal computer 1 Dimension) software. Initially single junction PIN structures are designed, followed by tunnel junctions and then multijunction PIN structure with tunnel junction as interfaces. A mathematical model is used to analyse the parameters of the device structure embedded in the PC1D. The flow of the methodology followed in this design is shown in fig. 1.

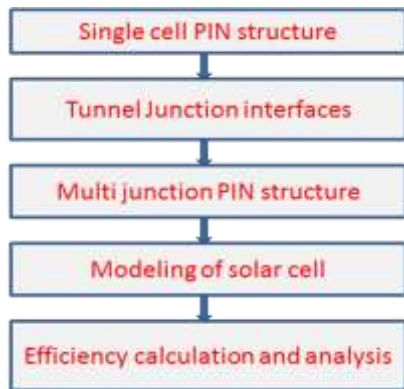


Fig. 1. Methodology adopted in the design and analysis of Quad Junction device

2.1. Proposed Cell structure

The model is a quad layer structure with a bottom layer, two middle layers and a top layer with anti reflective coating over it. The model is as shown below in fig.2

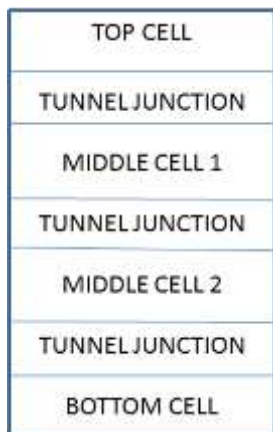


Fig. 2. Proposed Quad junction structure

The material used to make the cell layers is Indium Gallium Nitride and for tunnel junction, Gallium Nitride is used. The cell structure is built in PC1D, with parameters numerically modelled and specified in the software to build the individual layers of the cell. The cell is modelled with varied thickness of the layers for optimising the absorption. The spectrum made incident is AM1.5G spectrum with one sun intensity. The cell is structured in such a way that the thickness is lowered as a half of the previous layer thickness i.e. the top cell is structured with thickness of 10 μm, middle cell 1 with 5 μm, middle cell 2 to be 2.5 μm and bottom cell with 1.25 μm. The tunnel junction is a pn junction of 1μm thickness expect for the top and bottom cell, which has 0.05 μm for top n type layer and 0.01 μm for bottom p type layer.

2.2. Single junction Cell structure

To get high efficiency from a quad layer device, it is necessary to design and optimize the performance of single junction devices used for cascading. Hence, the four different single junction structures are designed and simulated separately to have knowledge of their cell parameters. The single junction structures from top to bottom with different grading concentrations

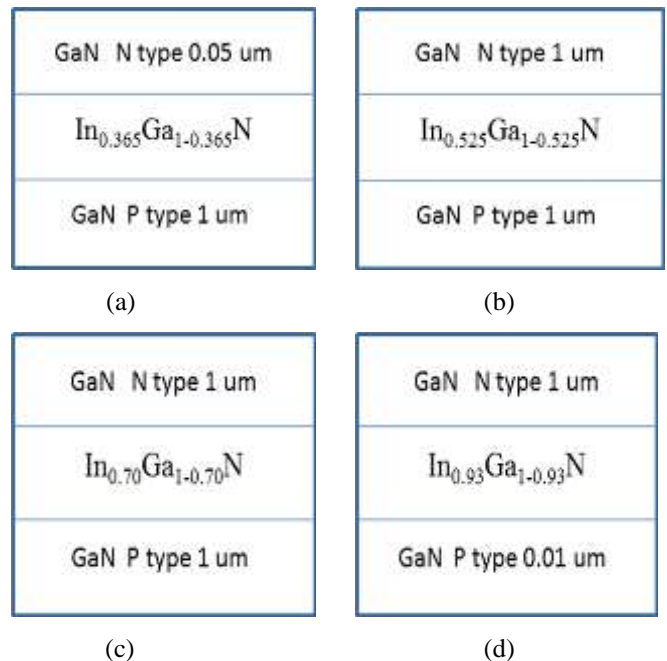


Fig. 3. Single junction structures of (a) top cell, (b) middle cell 1, (c) middle cell 2 and (d) bottom cell.

Fig. 3 (a, b, c & d) show the individual cell with the type of doping material and tunnel junction thickness. The thickness of the cell with intrinsic type InGaN is decreased by factor of half of the thickness of the previous InGaN layer. The doping concentrations to be considered for simulation are 5×10^{19} for n type doping and 3×10^{18} for p type doping of the GaN junction. As GaN is used for tunnelling the maximum number of charge carriers along the area of the cell, current mismatching still occurs at the junction. InGaN/GaN current mismatched structure holds potential consideration because of the lattice matching property of GaN. Calculation of the parameters required for simulation

such as band gap, electron affinity, refractive index, density of states for conduction band and valance band, dielectric constant, intrinsic concentration are numerically modelled and the values obtained for individual cells are shown in table 1.

Table 1. Numerically modelled parameters for individual cell structure

Cell	Top	Middle 1	Middle 2	Bottom
Band gap (eV)	1.405	1.804	2.324	3.141
Electron Affinity	21.204	19.54	17.72	15.328
Refractive index	2.137	2.674	3.005	2.963
Dielectric constant	21.204	19.54	17.72	15.328

2.3. Cascaded Quad junction structure

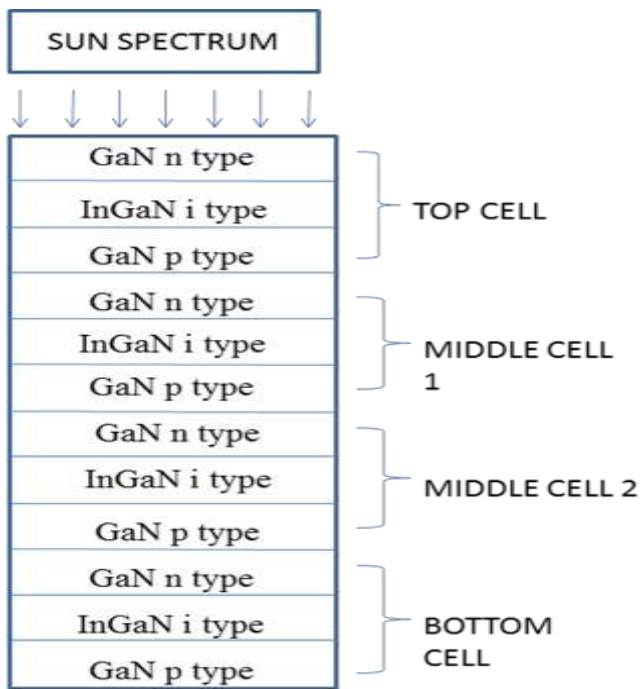


Fig. 4. Quad junction cascaded structure

The complete quad junction structure is shown in fig. 4. Cascading of 4 junctions together is not directly possible in PC1D, therefore two dual junctions are numerically cascaded together. i.e. top and middle 1 are cascaded as dual junction 1 and middle 2 and bottom cell are cascaded as dual junction 2 using the simulation software. Later, dual junction 1 and dual junction 2 are numerically cascaded together to obtain the voltage and current. The short circuit current, open circuit voltage and output power of the cascaded dual junctions are expressed as follows.

$$\text{Current}_{sc} = \min (\text{dual junction 1, dual junction 2})$$

$$\text{Voltage}_{oc} = V_{\text{dual junction 1}} + V_{\text{dual junction 2}}$$

$$\text{Output Power} = W_{\text{dual junction1}} + W_{\text{dual junction2}}$$

3. Simulation and Result analysis

Initially the individual solar cell structures are designed in the PC1D and simulated under AM1.5G one sun illumination. The simulated results obtained for the single junction structures like energy band diagram, generation & recombination rates and power- current -voltage characteristics are shown and analysed below in this section.

3.1. Energy band diagram of Single junction solar cells

The energy band diagram shows the conduction band energy level (E_C), valence band energy level (E_V), Intrinsic energy level (E_i) and fermi energy level (E_F). The difference between the conduction band and valence band energy level would give the energy band gap (E_g). In the fig. 5(a), the different energy levels of top cell is shown. It indicates E_C of 0.4 eV till 10 μm distance then rises to 1.6 eV. E_V varies from -1 eV at 10 μm to -1.8 eV thereafter. The energy band gap of the top cell results in 1.4 eV.

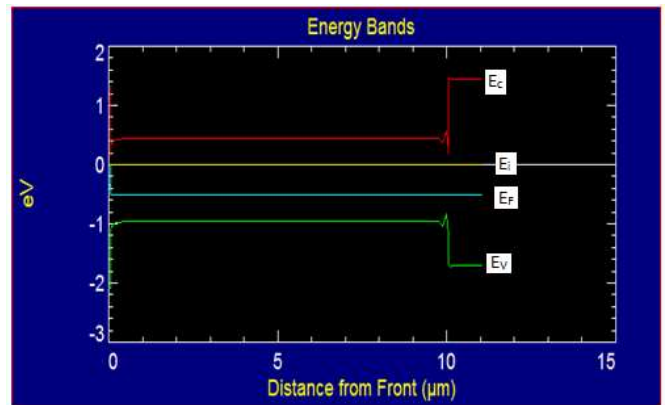


Fig. 5(a). Energy band diagram of top cell

In the fig. 5(b), the energy band diagram of middle cell 1 is shown. It showed an energy band gap of 1.8 eV from 0.4 μm to 6 μm distance. The fermi level lied at -0.5 eV in between the conduction and valence band.

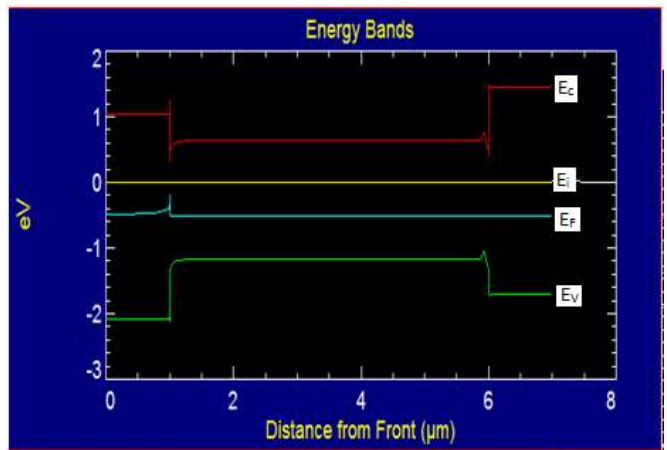


Fig. 5(b). Energy band diagram of Middle cell 1

In fig.5(c), the energy band diagram of the middle cell 2 is shown. This showed E_C at 0.8 eV from 1 μm to 3.4 μm and then varied. Similarly E_V showed a value of -1.5 eV in the range of 1 to 3.4 μm . The net energy band gap resulted in 2.3 eV that is close to the numerically solved result.

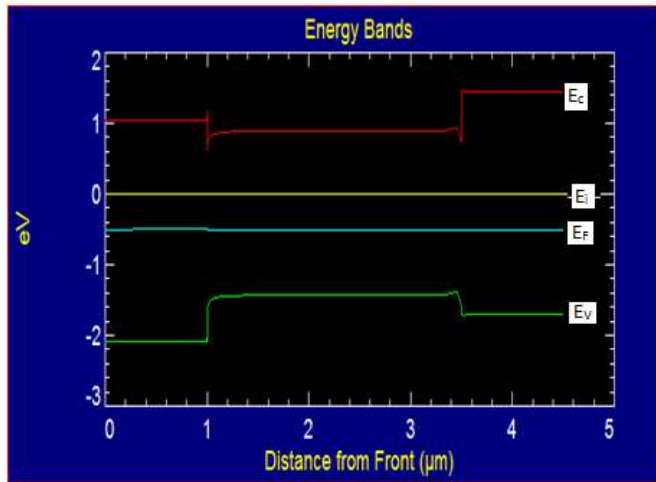


Fig. 5(c). Energy band diagram of Middle cell 2

Fig. 5(d) is the energy band diagram of the bottom cell, in which an energy band gap of 3.1 eV is resulted. Here E_C is at 1 eV and E_V at -2.1 eV.

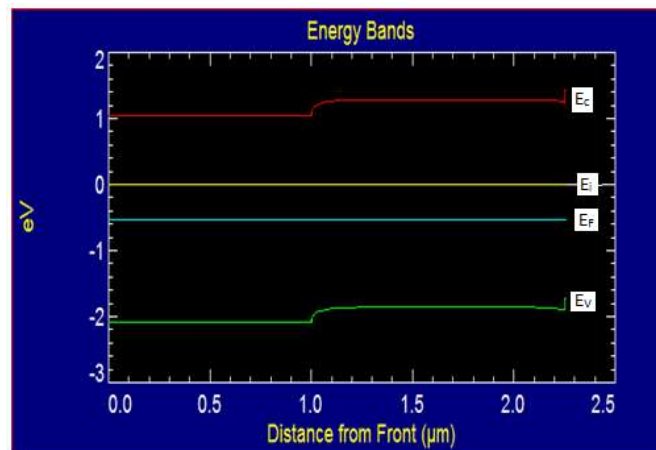


Fig. 5(d). Energy band diagram of Bottom cell

3.2. Generation and Recombination of Single junction solar cells

The generation and recombination rates prevailed in the different single junction solar cells during simulation are shown in fig. 6(a to d). The rate of generation in the top cell is accounted for $7 \times 10^{21}/\text{s}$ whereas the recombination is negligibly small. In the middle cell 1, the charge carriers are generated at the rate of $135 \times 10^{18}/\text{s}$ and recombined at $18 \times 10^{18}/\text{s}$. In the Middle cell 2, generation rate is $200 \times 10^{18}/\text{s}$ and recombination rate is $20 \times 10^{18}/\text{s}$. Finally in the bottom cell, the generation and recombination are $24 \times 10^{18}/\text{s}$ and $15 \times 10^{18}/\text{s}$. In the fig. 6 (a to d), the generation rates are shown in green whereas recombination is shown in red. It showed that maximum generation occurs in the middle cells 1 & 2, and reduced recombination in top and bottom cells.

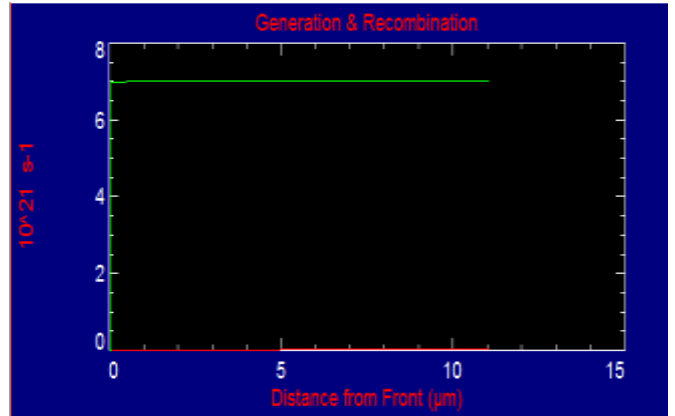


Fig. 6(a). Generation and recombination of top cell

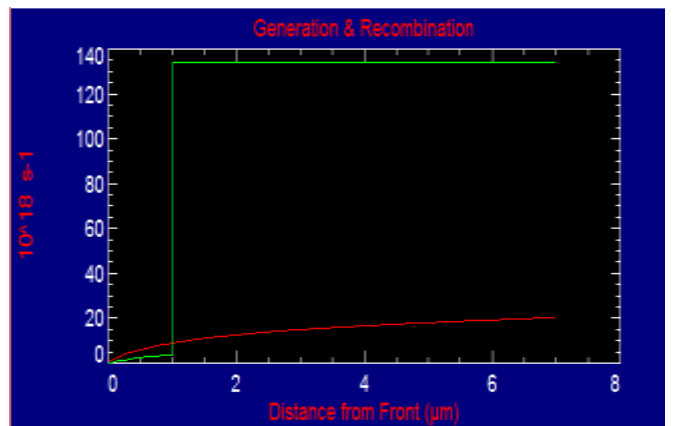


Fig. 6(b). Generation and recombination of middle cell1

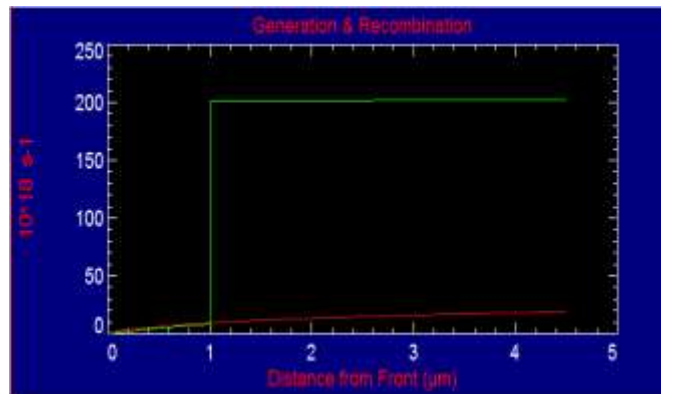


Fig. 6(c). Generation and recombination of middle cell2

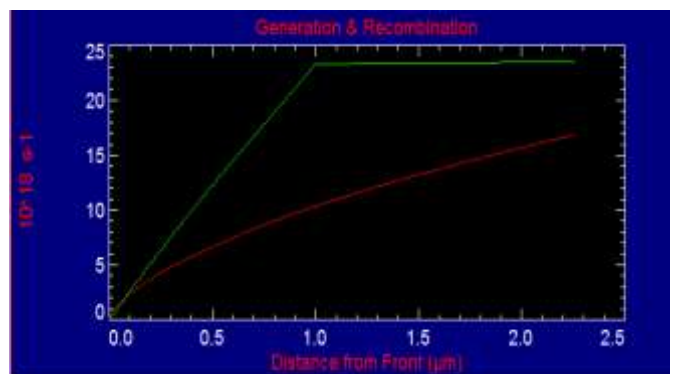


Fig. 6(d). Generation and recombination of bottom cell

3.3. Power- Current - Voltage curve of Single junction solar cells

The voltage vs current and voltage vs power curve of the cell is an important measure to determine the characteristics of cell. Accordingly the PIV curves obtained for the different single junction solar cells are shown in fig. 7(a to d). The different characteristics like open circuit voltage, short circuit current, rated power and fill factor are obtained from the figures. Using the available data, efficiency of the cell can be computed for one sun illumination. The observed results are shown in table 2.

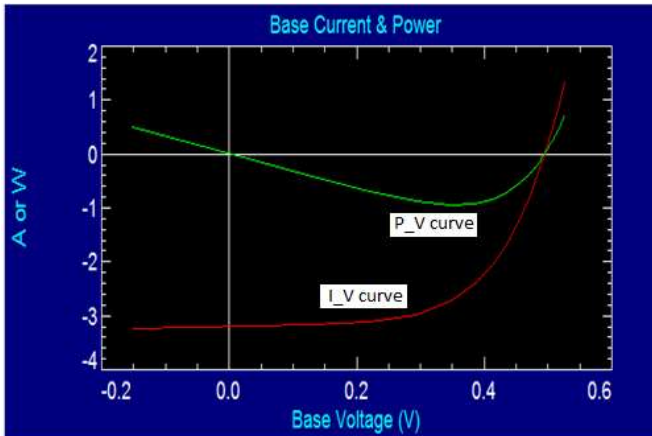


Fig. 7(a). PIV curve of top cell

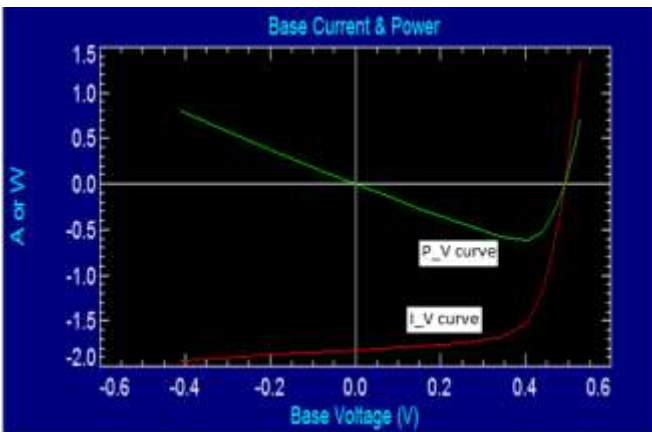


Fig. 7(b). PIV curve of middle cell 1

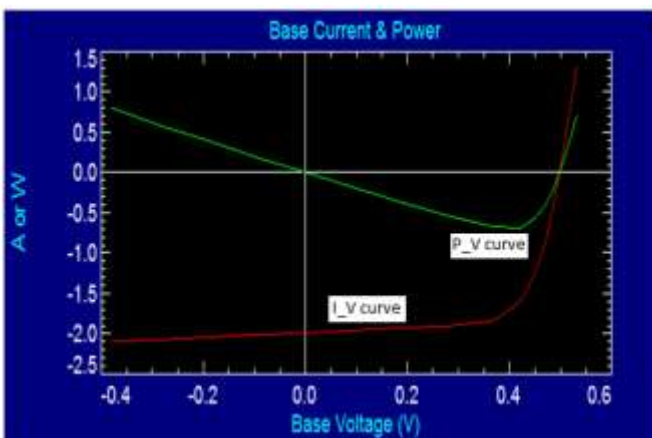


Fig. 7(c). PIV curve of middle cell 2

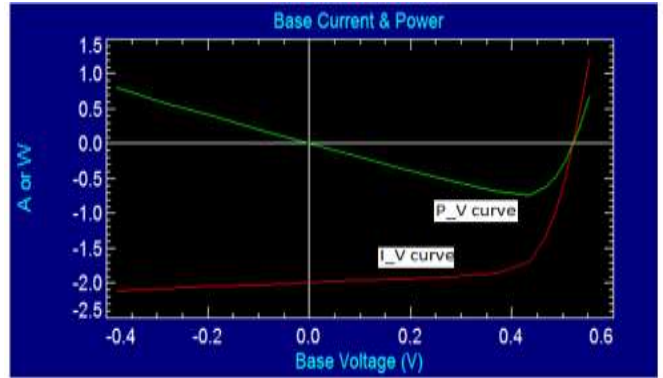


Fig. 7(d). PIV curve of bottom cell

Table 2. Characteristics of Single junction solar cells

Cells	V _{oc} (V)	I _{sc} (mA/cm ²)	P _{max} (W/cm ²)
Top	0.49	3.2	0.9
Middle 1	0.5	1.8	0.7
Middle 2	0.5	2.1	0.7
Bottom	0.5	2	0.6

3.4. Energy band diagram of Dual junction solar cells

There are two dual junction solar cells are designed using top and middle cell 1 as one dual junction, then middle cell 2 and bottom cell as another dual junction solar cell. The cascaded dual junction structures are simulated to get the characteristics of the solar cell. The energy band diagram and PIV curve of those dual junctions are shown below.

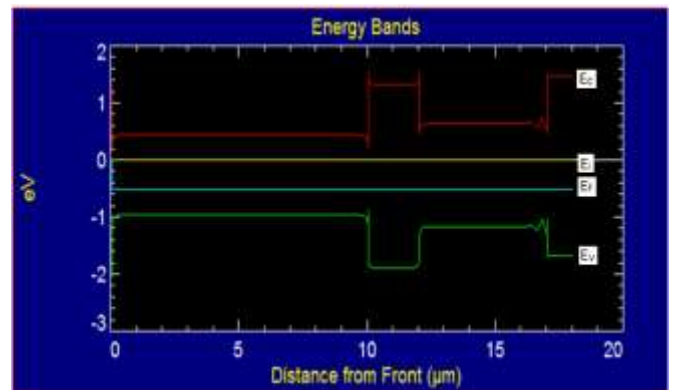


Fig. 8(a). Energy band diagram of Dual cell 1

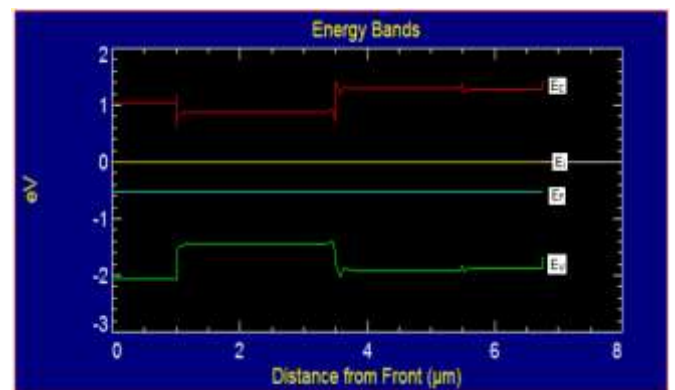


Fig. 8(b). Energy band diagram of Dual cell 2

The energy band diagram of the dual cell 1 is shown in fig. 8(a). E_C showed a value of 0.4 eV from (0 – 10) μm , 1.4 eV from (10 – 12) μm , 1.6 eV from (12-17) μm and 1.4 eV from (17-20) μm . E_V showed -1 eV from (0 – 10) μm , -1.8 eV from (10 – 12) μm , -1.2 eV from (12-17) μm and -1.8 eV from (17-20) μm . The band gap varies from 1.4 eV to 3.2 eV within the distance of 1 to 20 μm . In the fig. 8(b), the E_C showed a value of 1 eV from (0 – 1) μm , 0.8 eV from (1 – 3.5) μm and 1.4 eV from (3.5 -7) μm . E_V showed -2 eV from (0 – 1) μm , -1.4 eV from (1 – 3.5) μm and -1.8 eV from (3.5-7) μm . The band gap varies from 2.2 eV to 3.2 eV within the distance of 1 to 7 μm .

3.5. Energy band diagram of Dual junction solar cells

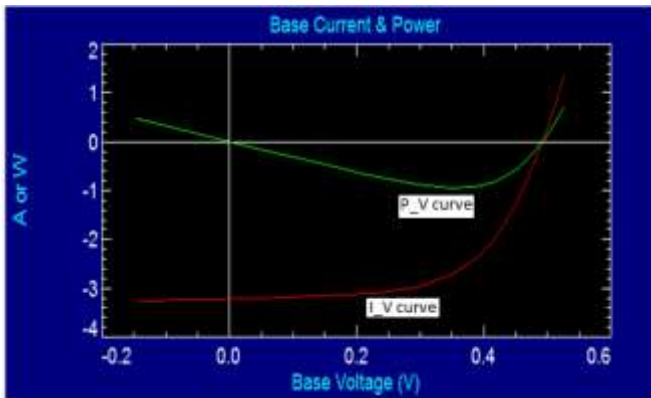


Fig. 9(a). PIV curve of Dual cell 1

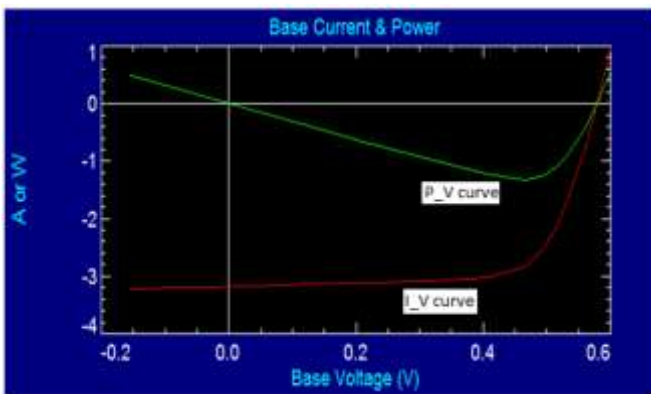


Fig. 9(b). PIV curve of Dual cell 2

The PIV curve of the dual junction solar cells are shown in fig. 9(a & b). The first dual junction cell has an open circuit voltage of 0.5 V, short circuit current of 3.2 mA/cm² and rated power of 0.9 W/cm². The second dual cell has an open circuit voltage of 0.58 V, short circuit current of 3.2 mA/cm² and rated power of 1.2 W/cm².

Then both the dual junctions are combined and simulated to get the results of a quad junction solar cell. The average results obtained from the single, dual and quad junction solar cells are shown in table 3. The average efficiency obtained from single junction cell is around 12%, dual junction cell is around 15 % and quad junction cell is around 33 %. A comparison of the proposed quad junction solar cell with other InGaN PIN solar cell is compared in table 4.

Table 3. Characteristics of proposed Different junction solar cells

Junction	Single	Dual	Quad
V _{oc} (V)	0.4946	0.5303	1.1799
I _{sc} (mA/cm ²)	3.197	3.231	3.181
Power (W/cm ²)	0.9514	1.342	2.3087
Fill factor (%)	80.18	82.90	89.62
Efficiency (%)	12.67	15.39	33.63

Table 4. Comparison of proposed quad junction solar cell with reference cell [28]

Cells	V _{oc} (V)	I _{sc} (mA/cm ²)	FF (%)	η (%)
Proposed cell	1.18	3.181	89.62	33.63
Reference cell	2.95	3.0	81.01	33.86

4. Conclusion

In this paper a quad PIN junction solar cell with InGaN material has been designed and simulated using PC1D. Thickness optimisation is done for degradation factor as function of half of the thickness of InGaN layers with tunnel junction thickness to be constant, for which the obtained efficiency is close to 34% for 100cm² area cell with fill factor of 0.892 and current of 3.181 mA/cm² and voltage to be 1.1799 V. This can be concluded that the thickness of the bottom cell should be kept very low for maximum current matching, and hence making it less sensitive to the defects between the layers. The simulation should be carried out for high values of bulk recombination as it facilitates high voltage output.

References

- [1] L. Siyu, and Q. Xiaosheng, “AlGaAs/GaAs tunnel junctions in a 4-J tandem solar cell”, IEEE transactions on Journal of Semiconductors, Vol. 32, No. 11, pp. 1120031 – 1120034, 2013.
- [2] C.G. Bailey, D.V. Forbes, S.J. Polly, Z.S. Bittner, Y. Dai, C. Mackos, and S.M. Hubbard, “Open circuit voltage improvement of InAs/GaAs quantum dot solar cells using reduced InAs coverage”, IEEE transactions on Journal of Photovoltaics, Vol. 2, No. 3, pp. 269-275, 2012.
- [3] M.W. Wiemer, H.B. Yuen, V.A. Sabnis, M.J. Sheldon, and I. Fushman, U.S. Patent Application No. 12/819, 534, 2010.
- [4] J.Y. Chang, S.H. Yen, Y.A. Chang, and Y.K. Kuo, “Simulation of high efficiency GaN/InGaN PIN solar cell with suppressed polarization and barrier effects”, IEEE Journal on Quantum Electronics, Vol. 49, No. 1, pp.17-23, 2013.
- [5] J. Y. Chang, and Y.K. Kuo, “ Numerical study on the influence of piezoelectric polarization on the performance

- of p-on-n (0001)-face GaN/InGaN PIN solar cells”, IEEE transactions on Electron Device Letters, Vol. 32, No. 7, pp. 937-939, 2011.
- [6] Y.K. Kuo, J.Y. Chang, and Y.H. Shih, “ Numerical study of the effects of hetero-interfaces, polarization charges, and step-graded interlayers on the photovoltaic properties of (0001) face GaN/InGaN PIN solar cell”, IEEE transactions on Journal of Quantum Electronics, Vol. 48, No. 3, pp. 367-374, 2012.
- [7] M. AVM, S. Kumar, and S. Prince, “Performance Estimation on Conversion Efficiency of Heterojunction with Intrinsic Thin layer (HIT) Solar cell by PC1D simulation”.
- [8] A. Asgari, and K. Khalili, “Temperature dependence of InGaN/GaN multiple quantum well based high efficiency solar cell”, Solar Energy Materials and Solar Cells, Vol. 95, No. 11, pp. 3124-3129, 2011.
- [9] J.P. Shim, S.R. Jeon, Y.K. Jeong, and D.S. Lee, “ Improved Efficiency by using transparent contact layers in InGaN-based PIN solar cells”, IEEE transactions on Electron Device Letters, Vol. 31, No. 10, pp. 1140 – 1142, 2010.
- [10] J.Y. Chang, Y.K. Kuo, “ Simulation of N-face InGaN based PIN solar cells”, Journal of Applied Physics, Vol. 112, No. 3, pp. 033109-033112, 2012.
- [11] G.F. Brown, J.W. Ager, W. Walukiewicz, and J. Wu, “ Finite element simulations of compositionally graded InGaN solar cells”, Solar Energy Materials and Solar cells, Vol. 94, No. 3, pp. 478-433, 2010.
- [12] L.H. Hsu, C.C. Lin, M.H. Tan, Y.L. Yeh, D.W. Lin, H.V. Han, and H.C. Kuo, “ Embedded InN dot-like structure within InGaN layers using gradient-Indium content in nitride based solar cell”, IEEE conference on Photovoltaic Specialists Conference (PVSC), pp. 2428-2431, 2013.
- [13] C.A. Fabien, M. Moseley, B. Gunning, W.A. Doolittle, A.M. Fischer, Y.O. Wei, and F.A. Ponce, “ Simulations, Practical limitations, and Novel Growth Technology for InGaN- based Solar cells”, IEEE Journal of Photovoltaics, Vol. 4, No. 2, pp. 601-606, 2014.
- [14] C. A. Fabien, B.P. Gunning, J.J. Merola, E.A. Clinton, and W.A. Doolittle, “Large –area III-nitride Double Heterojunction Solar cells with record – high in content InGaN absorbing layers”, 42nd IEEE Photovoltaic Specialist Conference, pp. 1-3, 2015.
- [15] C.A. Fabien, and W.A. Doolittle, “Guidelines and limitations for the design of high efficiency InGaN single junction solar cells”, Solar Energy Materials and Solar cells, Vol. 130, pp.354-363, 2014.
- [16] M.F. Cansizoglu, S. M. Hamad, D.P. Norman, F.Keles, E. Badraddin, T. Karabacak, and H.W. Seo, “ PIN InGaN nanorod solar cells with high short circuit current”, Applied Physics Express, Vol. 8, No. 4, pp. 042302-042306, 2015.
- [17] J.R. Dickerson, K. Pantzas, A. Ougazzaden, and P.L. Voss, “ Polarization –induced electric fields make robust n-GaN/i-InGaN/p-GaN solar cells”, IEEE transactions on Electron Device letters, Vol. 34, No. 3, pp. 363-365, 2013.
- [18] G. Giannoccaro, and V.M. Passaro, “ Analysis and simulation of superlattice GaN/InGaN PIN solar cells”, International Congress on Energy efficiency and Energy Related Materilas (ENEFM2013), pp.99-105, Springer International publishing, 2014.
- [19] O. Jani, M. Pramila, B. Sanjay Kumar, R. Abhijit, and D. Chenna, “P-GaN/i-InGaN/n-GaN Solar cell with In compositional grading”, Optical and Quantum Electronics, ISSN 0306-8919.
- [20] Y.K. Kuo, Y.A. Chang, H.W. Lin, J.Y. Chang, S.H. Yen, F.M. Chen, and Y.H. Chen, “ Advantages of InGaN solar cells with p-doped and high-Al-Content superlattice AlGaIn barriers, IEEE Photonics Technology letters, Vol. 25, No.1, pp. 85-87, 2013.
- [21] Y.S. Chen, C.H. Liao, C.T. Kuo, R.C.C. Tsiang, and H.C. Wang, “ Indium droplet formation in InGaN thin films with single and double heterojunctions prepared by MOCVD”, NANoscale research letters, Vol. 9, No.1, pp. 1-12, 2014.
- [22] S.W. Feng, C.M. Lai, C.Y. Tsai, Y.R. Su, and L.W. Tu, “ Modelling of InGaN pn junction solar cells”, Optical Materials Express, Vol.3, No.10, pp. 1777-1788, 2013.
- [23] W.J. Aziz, and K. Ibrahim, “ Study of design (In_{0.04}Ga_{0.96}N/SiC) solar cells”, Optoelectronics and Advanced materials rapid communications, Vol. 5, No.1, pp.12-15, 2011.
- [24] N. Akter, “ Design and Simulation of Indium gallium nitride multijunction tandem solar cells, International Journal of Renewable Energy technology, Vol.3, pp. 315-321, 2014.
- [25] D.J. Seo, J.P. Shim, S.B. Choi, T.H. Seo, E.K. Suh, and D.S. Lee, “Efficiency improvement in InGaN based solar cells by Indium tin oxide nano dots covered with ITO films”, Optics express, Vol.20, No.106, pp.A991-996, 2012.
- [26] R.H. Horng, S.T. Lin, Y.L. Tsai, M.T. chu, W.Y. Liao, M.H. Wu and Y.C. Lu, “ Improved conversion efficiency of GaN/InGaN thin film solar cells, IEEE Electron Device letters, Vol. 30, No. 7, pp. 724-726, 2009.
- [27] M.J. Jeng, Y.L. Lee, and L.B. Chang, “Temperature dependences of In_xGa_{1-x}N multiple quantum well solar cells”, Journal of Physics D: Applied physics, Vol. 42, No. 10, pp. 105101-105104, 2009.
- [28] J.Y. Chang, S.H. Yen, Y.A. Chang, B.T. Liou, and Y.K. Kuo, “ Numerical Investigation of high efficiency InGaN based multijunction solar cell”, IEEE transactions on Electron Devices, Vol. 60, No.12, pp. 4140-4145, 2013.